# Magnetohydrodynamic stability of tokamak edge plasmas

J. W. Connor, R. J. Hastie, H. R. Wilson, and R. L. Miller

Citation: Phys. Plasmas **5**, 2687 (1998); doi: 10.1063/1.872956
View online: http://dx.doi.org/10.1063/1.872956
View Table of Contents: http://pop.aip.org/resource/1/PHPAEN/v5/i7
Published by the American Institute of Physics.

# Magnetohydrodynamic stability of tokamak edge plasmas

J. W. Connor, R. J. Hastie, and H. R. Wilson
*UKAEA Fusion, Culham Science Centre, Abingdon, Oxon OX14 3DB, United Kingdom*

R. L. Miller
*General Atomics, San Diego, California 92186-5608*

(Received 3 December 1997; accepted 17 April 1998)

A new formalism for analyzing the magnetohydrodynamic stability of a limiter tokamak edge plasma is developed. Two radially localized, high toroidal mode number $n$ instabilities are studied in detail: a peeling mode and an edge ballooning mode. The peeling mode, driven by edge current density and stabilized by edge pressure gradient, has features which are consistent with several properties of tokamak behavior in the high confinement ''H''-mode of operation, and edge localized modes (or ELMs) in particular. The edge ballooning mode, driven by the pressure gradient, is identified; this penetrates $\sim n^{1/3}$ rational surfaces into the plasma (rather than $\sim n^{1/2}$, expected from conventional ballooning mode theory). Furthermore, there exists a coupling between these two modes and this coupling provides a picture of the ELM cycle. [S1070-664X(98)04007-5]

## I. INTRODUCTION

The edge region of the plasma is thought to have a strong influence on the performance of a tokamak as a whole. For instance, the marked improvement in confinement which is usually observed when the plasma makes the transition from the low confinement L-mode to the high confinement H-mode as the heating power is raised above a certain threshold appears to be due to changes in the edge region. At this transition, an increase in the radial electric field shear at the edge is observed[1] (caused by a spontaneous increase of plasma flow) and this is thought to decorrelate the plasma turbulence, thus reducing the thermal and particle diffusivities to generate a transport barrier.[2] The pressure gradient is increased in this transport barrier, so that the pressure rises steeply in from the edge up to a so-called ''pedestal'' value. Turbulent transport models for the core confinement (the core is defined to be the region on the inner side of the transport barrier region) can be very sensitive to the size of this pedestal (e.g., Ref. 3) and it is therefore an important ingredient in the prediction of the performance of future tokamaks, such as the International Thermonuclear Experimental Reactor (ITER).[4]

To model the edge pedestal, one requires two basic ingredients: the width of the transport barrier and the size of the pressure gradient in the barrier region. To determine the width of the barrier requires a knowledge of the mechanism responsible for its formation (e.g., what causes the plasma to spin up at the L–H transition, and over what radial region). To determine the size of the pressure gradient requires an understanding of the edge localized modes (ELMs) which are observed to limit it. While many mechanisms have been proposed for the plasma spin-up, relatively little attention has been given to the problem of analyzing localized edge instabilities. The latter is the main focus for this work.

Often the edge pressure gradient is assumed to be limited by the ideal magnetohydrodynamic (MHD) ballooning mode, and experimentally it is often comparable to the marginal stability value calculated from conventional ballooning theory.[5–7] However, conventional ballooning theory[8] cannot be applied at the plasma edge because the associated expansion in large toroidal mode number, $n$, is not then consistent. To illustrate the problem, it is worthwhile summarizing the conventional ballooning mode expansion procedure. Starting from the ideal MHD equations, an eigenmode equation is derived whose eigenvalue is the square of the mode frequency. This equation is a two-dimensional partial differential equation in the radial and poloidal angle coordinates and is difficult to solve numerically for large $n$, when the mode becomes radially localized, because of the need to resolve both the rapid radial variations associated with the mode structure and the slow radial variations associated with the equilibrium. However, under certain conditions a consistent ordering can be developed by expanding in powers of $n^{-1/2}$, which reduces the partial differential equation to a sequence of ordinary differential equations which are easier to solve numerically. First, use is made of the ballooning transform,[8] which maps the poloidal angle $\theta$ (defined on $[-\pi,\pi]$) onto the ballooning angle $\eta$ (defined on $[-\infty,\infty]$): this allows one to replace the periodicity boundary condition in $\theta$ with boundary conditions at $\eta=\pm\infty$ and to express the ballooning-transformed eigenfunction in eikonal form [i.e., as the product of an amplitude $F(\psi,\eta)$ and an eikonal $\exp(-inS)$, where $\mathbf{B}\cdot\nabla S=0$ and $\psi$ is proportional to the poloidal flux which is used as a radial variable]. A two-dimensional (2-D) equation for $F$ in $\psi$ and $\eta$ results, which can be solved by developing an expansion in the small parameter $n^{-1/2}$. To leading order, a single ordinary differential ''ballooning equation'' is obtained, involving differential operators in $\eta$ along a field line. This defines a local eigenvalue, $\omega^2(\psi,k)$, which depends only weakly on $\psi$ through the radial variations in the equilibrium parameters that form the coefficients of the ballooning equation. The parameter $k$,

which represents a radial wave number associated with the eikonal $S$, is not determined at this order. This parameter $k$, the radial structure (or ''envelope'') of the mode and the relation between the local eigenvalue $\omega^2$ and the true, global eigenvalue $\Omega^2$, are all determined at higher order. The position in the plasma of particular interest is that which is most unstable, i.e., where $\omega^2$ is a minimum. If this minimum occurs in the plasma core (say at $\psi=\psi_0$), then $\partial\omega^2/\partial\psi|_{\psi=\psi_0}=0$ there, and $\omega^2$ can be expanded in a Taylor series in $(\psi-\psi_0)$, keeping only the constant term $\omega^2(\psi_0)$ and the quadratic term. One can then develop the expansion in $n^{-1/2}$: a solubility condition at $O(n^{-1/2})$ determines $k$ through the relation $\partial\omega^2/\partial k=0$, while the $O(n^{-1})$ equation determines the radial envelope function, and yields $\Omega^2=\omega^2(\psi_0,k)+O(n^{-1})$. Thus the stability properties for the ideal MHD ballooning mode can be obtained purely from the eigenvalues $\omega^2(\psi_0,k)$ of the leading order ballooning equation; however, the key results $\partial\omega^2/\partial k=0$ and $\Omega^2\simeq\omega^2$ must hold, and therefore require that the higher order theory is consistent. This is the crucial point: At the edge of the plasma the higher order theory, developed as an expansion in $n^{-1/2}$, is *not* consistent. The new aspect is that when the most unstable position in the plasma (as determined from the local eigenvalue $\omega^2$) is at the plasma edge, $\partial\omega^2/\partial\psi\neq 0$ (in general); thus the Taylor expansion of $\omega^2(\psi)$ must retain terms linear in $\psi-\psi_0$ and the higher order equations in the $n^{-1/2}$ expansion are then inconsistent.

There is a second issue related to MHD stability at the plasma edge. Associated with the edge is the potential for a localized high $n$ kink, or ''peeling,'' mode driven by an edge current density.[9,10] Typically there will always be a finite current density at the plasma edge, either due to a finite edge temperature (so that an Ohmic current flows) or due to a finite edge pressure gradient, in which case the Pfirsch–Schlüter and bootstrap currents[11] may also contribute. This mode has features which make it a prime candidate for explaining both the improved performance and ease of access to H-mode which occurs when the current is ramped down during a tokamak discharge (such a ramp-down transiently reduces the current density at the relatively cool edge).[12]

In this paper we look in more detail at these edge stability issues, concentrating on high $n$ modes and restricting ourselves to a limiter plasma configuration for simplicity. In the following section we review the status of the peeling mode stability theory, which provides a necessary stability criterion for the mode; this is analagous to the Mercier criterion for localised internal modes.[13] For general axisymmetric toroidal geometry, this peeling mode stability condition is

$$\sqrt{1-4D_M}>1+\frac{2}{2\pi q'}\oint\frac{j_\parallel B}{R^2B_p^3}\,dl, \tag{1}$$

where $D_M$ is the Mercier index (i.e., the Mercier stability criterion is $1-4D_M>0$), $q$ is the safety factor, $j_\parallel$ is the current density parallel to the magnetic field $\mathbf{B}$, $R$ is the major radius, $B_p$ is the poloidal magnetic field strength, $dl$ is a poloidal arc length element on a flux surface, and a prime denotes a derivative with respect to $\psi$ (defined to increase towards the plasma edge). All quantities are evaluated at the plasma edge. The fact that $D_M$ is proportional to the pressure gradient suggests that a high pressure gradient tends to stabilize the peeling mode when $D_M<0$, i.e., there is favorable average curvature, which we term a ''magnetic well.'' However, as we have already discussed, there are pressure gradient driven currents to be included on the right-hand side of Eq. (1): The bootstrap current is parallel to the magnetic field and is clearly destabilizing, while the Pfirsch–Schlüter current contribution is parallel to the field on the outboard side of the torus, and antiparallel on the inboard side. The role of the Pfirsch–Schlüter current requires a careful evaluation of the flux surface integral, which we perform in Sec. II for a large aspect ratio equilibrium with weak shaping. The result is that it is stabilizing, and comparable in magnitude to the effect of $D_M$. The implications of this are discussed further in Sec. II.

The theory described in Sec. II concerns modes which are radially localized on the scale associated with the distance between rational surfaces; ballooning structures which span many rational surfaces (though nevertheless are localized with respect to the equilibrium length scale) are not described by the stability criterion of Eq. (1): Eq. (1) therefore provides a necessary, but not sufficient, stability criterion. In Sec. III we employ a model MHD equation, based on the familiar ''$s-\alpha$'' model,[14] which has the key ingredients required for both ballooning and peeling modes: toroidal coupling, edge current density, magnetic well, etc. The original derivation of the $s-\alpha$ model neglected finite aspect ratio effects which would give rise to a magnetic well: We reintroduce the well as a parameter of the model. We use this model equation to illustrate the essential features of edge ballooning modes, by means of

(i) direct numerical solution;
(ii) a modified ballooning formalism, valid at the plasma edge.

In fact, exploiting insights gained from numerical solution of the model system, the new ballooning formalism can be applied to an arbitrary axisymmetric torus, provided the coupling to the peeling mode is neglected. One finds that edge MHD ballooning modes have similar stability properties to the conventional ballooning modes, but a quite different radial mode structure: one which spans $\sim n^{1/3}$ rational surfaces with a radial envelope that resembles the exponential tail of an Airy function[15] (rather than $\sim n^{1/2}$ surfaces with a Gaussian envelope, which is the result for the conventional ballooning modes).

We close in Sec. IV with a qualitative discussion of our results and their relevance to features observed on tokamaks. In this paper we concentrate on a limiter geometry, while nevertheless relating many of the results to tokamak behavior found in separatrix geometry. A natural extension of the work will be to develop the theory in a separatrix geometry and we discuss some of the challenging problems which need to be addressed to reach this goal.

## II. LOCALIZED PEELING STABILITY CRITERION

The stability of both the peeling and ballooning modes are based on the MHD energy principle. The peeling mode

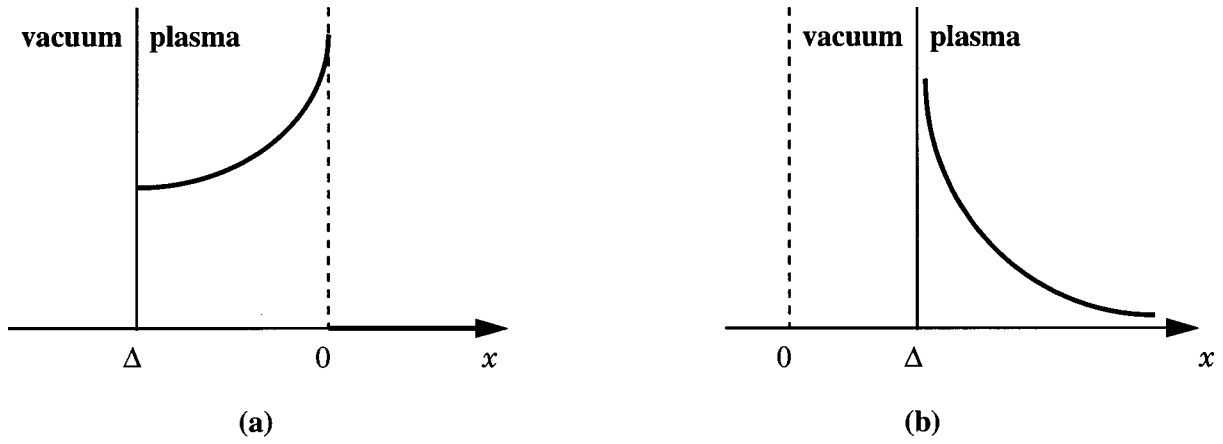


FIG. 1. The geometry for the localized peeling mode analysis, showing the form of the trial function in bold for (a) the rational surface (at $x=0$) inside the plasma and (b) the rational surface outside the plasma.

occurs when its resonant rational surface lies near the plasma surface, in which case the expression for the energy can be simplified. The calculation is given in the Appendix, where we repeat the derivation by Lortz of the change in energy associated with a localised surface mode.[9] (This Appendix also serves to define the MHD energy principle and some of the notation used.) By adopting trial functions for the radial plasma displacement, $\xi$, it is then possible to derive a necessary stability criterion for this mode.[10] In this section we describe the essential features of this stability criterion which will be used in Sec. III to compare with the numerical calculations.

The potential energy is

$$\delta W=\frac{\Delta^2}{2}\int_{\Delta}^{\infty}dx\left\{Px^2\left(\frac{d\xi}{dx}\right)^2+Q\xi^2+S\frac{d}{dx}(x\xi^2)\right\}, \quad (2)$$

where $x=\Delta$ represents the plasma edge, $x=0$ is the rational surface, and $x=\infty$ is deep in the plasma core. The geometry is illustrated in Fig. 1 and the equilibrium flux surface quantities $P$, $Q$, and $S$ are defined in Eq. (A23) of the Appendix. The Euler equation which minimises Eq. (2) is

$$\frac{d}{dx}\left(x^2\frac{d\xi}{dx}\right)-\frac{Q}{P}\xi=0 \quad (3)$$

with solutions

$$\xi=a_+x^{\lambda_+}+a_-x^{\lambda_-}, \quad (4)$$

where

$$\lambda_{\pm}=-\frac{1}{2}\pm\sqrt{\frac{1}{4}+\frac{Q}{P}}. \quad (5)$$

It is interesting to note that the Mercier coefficient $D_M \equiv -Q/P$ (Ref. 16 uses the notation $D_I=D_M-1/4$), and therefore the necessary stability criterion, that the solutions be nonoscillatory in $x$, is simply the Mercier criterion

$$D_M-\tfrac{1}{4}<0. \quad (6)$$

However, the existence of an edge current provides a more restrictive necessary stability criterion. There are two situations of interest: (a) when the rational surface is inside the plasma (in which case $\Delta<0$) and (b) when it is outside (see Fig. 1).

Consider first the situation when the rational surface is inside the plasma, and choose a trial function which is zero for $x>0$ and satisfies the Euler Eq. (3) for $\Delta<x<0$ [see Fig. 1(a)]. This effectively replaces the upper integration limit of $\delta W$ with 0, so that for $\delta W$ to be finite we must choose $a_-=0$. The result for $\delta W$ is that

$$\delta W=-\frac{1}{2}P|\Delta|^{2\lambda_++2}\Delta\left[\frac{S}{P}+\lambda_+\right] \quad (7)$$

so that stability requires

$$\sqrt{1-4D_M}>1-2\frac{S}{P}. \quad (8)$$

We turn now to the situation when the rational surface is outside the plasma. We are only interested in the form of $\xi$ within the plasma, so we select the solution to the Euler equation which is well-behaved as $x\to\infty$; i.e., we set $a_+=0$. Thus in this situation we find

$$\delta W=-\frac{1}{2}P\Delta^{2\lambda_-+3}\left[\frac{S}{P}+\lambda_-\right] \quad (9)$$

and stability requires

$$\sqrt{1-4D_M}>2\frac{S}{P}-1. \quad (10)$$

Combining Eqs. (8) and (10) (since both must be satisfied for stability) and recalling the definitions of $S$ and $P$ [Eq. (A23)], the stability criterion for the usual tokamak case, $j_{\|}>0$, becomes

$$\sqrt{1-4D_M}>1+\frac{2}{2\pi q'}\oint\frac{j_{\|}B}{R^2B_p^3}\,dl, \quad (11)$$

where all quantities are to be evaluated at the plasma surface. This illustrates the destabilizing nature of the edge parallel current density when it is in the same direction as the magnetic field. An interesting question concerns the role of the

Pfirsch–Schlüter current, which is parallel to the magnetic field on the outboard side and antiparallel on the inboard side. This current can be expressed as

$$j_{\|}^{\mathrm{PS}} = -\frac{Ip'}{B}\left(1-\frac{B^2}{\langle B^2\rangle}\right), \tag{12}$$

where $I=RB_\phi$, with $B_\phi$ the toroidal magnetic field strength, and angled brackets denote the flux surface average

$$\langle\cdots\rangle = \frac{\oint\cdots dl/B_p}{\oint dl/B_p}. \tag{13}$$

Therefore, the Pfirsch–Schlüter current provides a contribution

$$-\frac{2Ip'}{2\pi q'}\oint\left(1-\frac{B^2}{\langle B^2\rangle}\right)\frac{1}{R^2B_p^3}\,dl \equiv -2H \tag{14}$$

to the right-hand side of Eq. (11), in the notation of Glasser, Greene, and Johnson.[17] Thus, continuing with this same notation, we can write the stability condition (11) as

$$\sqrt{\frac{1}{4}-E-F-H}-\frac{1}{2}+H>\frac{1}{2\pi q'}\oint\frac{\overline{j}_{\|}B}{R^2B_p^3}\,dl, \tag{15}$$

where now $\overline{j}_{\|}$ excludes the Pfirsch–Schlüter contribution. An interesting result is that for a large aspect ratio, low $\beta$ ordering ($\beta$ is the ratio of thermal energy to magnetic energy), for which $E,F,H\ll 1$, the right-hand side of Eq. (15) becomes equal to $-D_R$, where $D_R<0$ is a necessary condition for stability to resistive interchange modes,[16] i.e., the stability condition in this case can be written

$$D_R < -\frac{Rq}{s}\left(\frac{\overline{j}_{\|}}{B}\right)_{\mathrm{edge}}, \tag{16}$$

where $s=(r/q)(dq/dr)$ is the magnetic shear, $r$ is the minor radius, and $(j_{\|}/B)_{\mathrm{edge}}$ is positive when $\overline{j}_{\|}$ is in the direction of the magnetic field. Note that when an edge current exists this condition is more restrictive than the resistive interchange stability criterion ($D_R<0$). Expressions for $D_R$, including weak shaping, exist in the literature[18,19] and can simply be substituted into this expression. If the effects of shaping are neglected, the leading order stability condition can be written in terms of the radial derivative of the Shafranov shift, $\Delta'$

$$\alpha\left\{\frac{r}{R}\left(1-\frac{1}{q^2}\right)+s\Delta'-f_t\frac{Rs}{2r}\right\} > Rqs\left(\frac{j_{\|}^{\mathrm{driven}}}{B}\right)_{\mathrm{edge}}, \tag{17}$$

where the ballooning stability parameter[14]

$$\alpha = -2\frac{Rq^2}{B^2}\frac{dp}{dr} \tag{18}$$

characterizes the edge pressure gradient and $j_{\|}^{\mathrm{driven}}$ is the externally driven current (i.e., Ohmic plus auxiliary) with the bootstrap current *and* Pfirsch–Schlüter current subtracted. The term proportional to $(1-1/q^2)$ originates from $D_M$, while that proportional to $\Delta'$ originates from the Pfirsch–Schlüter current, and both effects are stabilizing for a large aspect ratio, weakly shaped tokamak equilibrium. The third term on the left-hand side stems from the bootstrap current contribution to $j_{\|}$ and is found to be destabilizing. The fraction of trapped particles is represented by $f_t\sim(r/R)^{1/2}$, in the banana collisionality regime, so that the bootstrap term is the dominant one [by $(R/r)^{3/2}$] on the left-hand side and instability is expected. At higher collisionality, when $f_t\to 0$, stability depends on the balance between the stabilizing pressure gradient terms (left-hand side) and the destabilizing edge current density (right-hand side). Thus one would expect the peeling mode to emerge at low edge collisionality, while for higher collisionality it can be stabilized by sufficiently high pressure gradient.

## III. EDGE BALLOONING MODES

The previous section was concerned with very localized edge modes at high $n$ (i.e., localized to less than the distance between mode rational surfaces) and neglected any effects due to toroidal coupling of ''internal'' Fourier modes localized about adjacent rational surfaces. This is known to be important in typical tokamak core conditions at high pressure, when $\sim n^{1/2}$ rational surfaces are coupled to give the so-called ballooning mode. In this section we investigate the modifications to the peeling mode due to toroidal coupling as the pressure gradient increases towards values corresponding to ballooning instability.

This paper is concerned with the essential features of edge mode structures and stability, which we illustrate with a simple model tokamak equilibrium that encompasses the features of the familiar $s-\alpha$ model originally employed to investigate core ballooning stability.[14] This equilibrium is based on a self-consistent low $\beta$ expansion of a circular, large aspect ratio tokamak equilibrium, but with the pressure gradient enhanced in a narrow radial region of interest (in this case, at the plasma edge).

To derive the edge MHD stability equations, we begin with the change in energy associated with a small plasma displacement

$$\delta W = \delta W_F + \delta W_S + \delta W_V, \tag{19}$$

where $\delta W_F$ is the change in energy associated with the plasma, integrated over the plasma volume, $\delta W_S$ is the energy change associated with the plasma surface, and $\delta W_V$ is the energy change associated with perturbations of the magnetic field in the vacuum region outside the plasma (the effect of any surrounding vessel is not important for these high $n$ modes). We begin with the plasma contribution, which can be derived from Eq. (A1) in a large $n$ expansion: Terms of $O(1/n)$ will be shown to be unimportant, and are therefore not retained here. Using the same variables as in the Appendix, we can express $\delta W_F$ in terms of $X$, related to the radial component of the plasma displacement, $\xi$

$$\delta W_F=\pi\int d\psi\, d\chi\, X^*\Bigg\{JBk_\parallel\Bigg[\frac{1}{JR^2B_p^2}\Bigg[1-\left(\frac{R^2B_p^2}{B}\right)^2\times\frac{1}{n^2}\frac{\partial^2}{\partial\psi^2}\Bigg]JBk_\parallel X\Bigg]+\frac{iIp'}{B^4}\frac{\partial B^2}{\partial\chi}\frac{1}{n}\frac{\partial X}{\partial\psi}-\frac{2Jp'}{B^2}\frac{\partial}{\partial\psi}\left(p+\frac{B^2}{2}\right)X\Bigg\},\tag{20}$$

which, not surprisingly, is the same result as that derived for core modes.[8] However, because the integral over $\psi$ extends to the plasma edge, the various integrations by parts used to derive Eq. (20) result in a number of surface terms, which constitute $\delta W_S$

$$\delta W_S=\pi\int d\chi\,\frac{X^*}{n}\,JBk_\parallel\left[\frac{R^2B_p^2}{JB^2}\frac{1}{n}\frac{\partial}{\partial\psi}(JBk_\parallel X)+\sigma X\right],\tag{21}$$

where the flux surface integral is taken over the plasma surface. We have introduced the parameter $\sigma$ which represents the edge current density parallel to the magnetic field: $\sigma=j_\parallel/B$.

Defining a ''straight field line'' angle $\theta$

$$\theta=\frac{1}{q}\int_k^\chi \nu\, d\chi,\tag{22}$$

where $k$ plays the role of a radial wave number, we Fourier decompose the radial displacement

$$X=\sum_m u_m(\psi)e^{-im\theta+in\phi}.\tag{23}$$

Anticipating later results, we restrict our attention to a radial distance extending over $\sim n^{1/3}$ rational surfaces from the plasma edge, and drop terms of $O(1/n)$ to derive

$$\delta W_F=\pi\sum_{m,m'}\int d\psi\int d\theta\, e^{-i(m-m')\theta}u_{m'}^*\Bigg\{(m'-nq)\times\Bigg[\frac{I}{R^4B_p^2q}\Bigg[1-\left(\frac{R^2B_p^2}{B}\right)^2\left(\frac{1}{n^2}\frac{\partial^2}{\partial\psi^2}-2iq\theta'\frac{1}{n}\frac{\partial}{\partial\psi}-(q\theta')^2\right)\Bigg](m-nq)u_m\Bigg]-\frac{q}{\nu}\frac{2Jp'}{B^2}\frac{\partial}{\partial\psi}\left(p+\frac{B^2}{2}\right)u_m+\frac{q}{\nu}\frac{Ip'}{B^4}\frac{\partial B^2}{\partial\chi}\left(\frac{i}{n}\frac{\partial}{\partial\psi}+q\theta'+\frac{(m-nq)}{n}\theta'\right)u_m\Bigg\}.\tag{24}$$

At this stage we consider a specific model equilibrium, based on the $s-\alpha$ model described above. For simplicity we drop the last term of Eq. (24) which, although formally of the same order as equilibrium radial variations (which are retained), adds little to the essential understanding of the nature of MHD stability at the plasma edge. We justify this as follows. In the next section we shall demonstrate that the largest distance covered by the modes of interest is $\sim n^{1/3}$ rational surfaces. This distance is determined by the small terms $\sim n^{-2/3}$ of Eq. (24) which vary with radius across the rational surfaces: The term which we drop is also $\sim n^{-2/3}$ but does not vary across rational surfaces, by which we mean it is invariant under the transformation $m\to m+1$ and $nq\to nq+1$, and it will not therefore affect the leading order mode structure. Thus, after integrating over the poloidal angle, we arrive at our final result for $\delta W_F$

$$\delta W_F=-\frac{2\pi^2B}{nq'R^3B_p^2q}\sum_m\int_\Delta^\infty dx\, u_m^*(x)\Bigg\{s^2(x-M)^2\frac{d^2u_m}{dx^2}+2s^2(x-M)\frac{du_m}{dx}-(x-M)^2u_m-\alpha\Bigg\{s\Bigg[(x-M)^2+\frac{1}{2}\Bigg]\times\frac{d}{dx}(u_{m+1}-u_{m-1})+s(x-M)\frac{d}{dx}(u_{m+1}+u_{m-1})+s(x-M)(u_{m+1}-u_{m-1})-\frac{1}{2}(u_{m+1}+u_{m-1})-d_mu_m\Bigg\}-\frac{\alpha^2}{2}\Bigg\{[(x-M)^2+1]\Bigg[u_m-\frac{1}{2}(u_{m+2}+u_{m-2})\Bigg]-(x-M)(u_{m+2}-u_{m-2})\Bigg\}\Bigg\}.\tag{25}$$

Here we have defined a ''shifted'' poloidal mode number $M=m_0-m$, where $m_0$ is the poloidal mode number of the first rational surface outside the plasma (i.e., $M$ increases into the plasma from the edge). We have also defined a new radial variable

$$x=m_0-nq\tag{26}$$

which also increases into the plasma from the edge. Thus $x=0$ is at the location of the first rational surface outside the plasma, while $x=\Delta$ defines the plasma edge [see Fig. 1(b)]. The pressure gradient parameter $\alpha$, familiar from ballooning theory,[14] couples different poloidal harmonics and also leads to a magnetic well, which can provide stability to peeling modes as described in Sec. II. We have introduced such a term through the parameter $d_m$, where $d_m$ is related to the Mercier coefficient introduced in the previous section

$$D_M=\frac{\alpha d_m}{s^2}.\tag{27}$$

A more accurate calculation to higher order in $\epsilon$, where $\epsilon\ll 1$ is the inverse aspect ratio, leads to $d_m\simeq\epsilon(q^{-2}-1)$; we have neglected the effects of shaping. Although formally this term is small in $\epsilon$ it does have a qualitative effect on the stability criterion. A further detail used in deriving Eq. (25) is that we

have redefined $k$ to absorb the $\sin k$ terms which arise from $\theta'$ defined in Eq. (22), so that for this equilibrium $k \to k + (\alpha/s)\sin k$.

The same expansion can be used to derive the form for the contribution of the surface term to the energy

$$\delta W_S = -\frac{2\pi^2}{nRq}\sum_m u_m^*(\Delta - M)\left[ s\frac{d}{dx}[(x-M)u_m] + \gamma u_m - \frac{\alpha}{2}(\Delta - M)(u_{m+1} - u_{m-1})\right]_{x=\Delta}, \tag{28}$$

where the edge current density along the magnetic field is now expressed in terms of the dimensionless parameter $\gamma = 2j_\parallel/\langle j\rangle$ ($\langle j\rangle$ is the average current density, the ratio of total plasma current to the poloidal cross-sectional area of the plasma); for the large aspect ratio, circular cross section plasma we are considering, $\gamma = 2 - s$. Finally, in the cylindrical approximation the vacuum contribution can also be expressed in terms of a surface term

$$\delta W_V = \frac{2\pi^2}{nRq}\sum_m (\Delta - M)^2 u_m^* u_m . \tag{29}$$

From Eq. (25) we can immediately write down the Euler equation which minimizes the plasma energy $\delta W_F$ with respect to variations in $u_m^*$

$$\begin{aligned} &s^2(x-M)^2\frac{d^2u_m}{dx^2} + 2s^2(x-M)\frac{du_m}{dx} - (x-M)^2 u_m \\ &\quad - \alpha\left\{ s\left[(x-M)^2 + \frac{1}{2}\right]\frac{d}{dx}[u_{m+1} - u_{m-1}]\right. \\ &\quad + s(x-M)\frac{d}{dx}[u_{m+1} + u_{m-1}] \\ &\quad + s(x-M)[u_{m+1} - u_{m-1}] \\ &\quad \left. - \frac{1}{2}[u_{m+1} + u_{m-1}] - d_m u_m\right\} - \frac{\alpha^2}{2}\left\{[(x-M)^2 + 1]\right. \\ &\quad \left.\times\left(u_m - \frac{1}{2}[u_{m+2} + u_{m-2}]\right) - (x-M)[u_{m+2} - u_{m-2}]\right\} \\ &= 0. \end{aligned} \tag{30}$$

The boundary conditions on this set of coupled differential equations are that $u_m(x) \to 0$, for all $m$, as $x \to \infty$ (i.e., deep in the plasma) and that the ''surface'' contributions (28) and (29) to the energy be zero (which then implies $\delta W = 0$, as required for marginal stability). Again, the surface terms are stationary with respect to variations in the surface values of $u_m^*$, provided

$$(\Delta - M)\left\{ -s(\Delta - M)\frac{du_m}{dx} - [2 - (\Delta - M)]u_m + \frac{\alpha}{2}(\Delta - M)(u_{m+1} - u_{m-1})\right\}_{x=\Delta} = \Omega^2 u_m , \tag{31}$$

which includes the contribution due to the vacuum energy, and $\gamma = 2 - s$ has been substituted. In addition, we have included an artificial ''kinetic energy'' term on the right-hand side, which simplifies the identification of the most unstable mode (i.e., that with lowest $\Omega^2$, where $\Omega$ plays the role of the mode frequency). We are interested in determining marginal stability conditions, for which $\Omega^2 = 0$.

As an aside, it is interesting to note that there are two alternative ways to derive the boundary condition equations. First, one can solve the Euler Eq. (30) and then the condition that the resulting eigenfunctions $u_m$ match those in the vacuum is simply Eq. (31). This can be seen by integrating Eq. (A18) of Ref. 20 across the plasma–vacuum interface, taking proper account of the discontinuities in pressure gradient and current density. A second technique is to take a set of linearly independent solutions to Eq. (30) which satisfy the boundary condition at $x \to \infty$, say $v_m^j(x)$. The $u_m(x)$ are constructed as linear combinations of these

$$u_m(x) = \sum_j a_j v_m^j(x), \tag{32}$$

where a set of equations for the coefficients $a_j$ are derived by substituting Eq. (32) into Eq. (28) and minimizing with respect to $a_j$. This approach gives the same stability boundaries as those derived later in this paper.

The system of equations (30) and (31) constitutes the model with which we analyze the stability and mode structure of peeling and ballooning modes. In the following subsections we solve this system of equations by (a) full 2-D numerical solution and (b) a ballooning solution when $\alpha$ is close to the ballooning stability boundary. Radial equilibrium variations are modeled by

$$\alpha = \alpha_a - \frac{\alpha_d}{nq_a s}(x - \Delta), \tag{33}$$

where the subscript $a$ signifies the edge value and we consider constant shear $s$ for simplicity; this is adequate for discussing the essentials of the radial mode structure. The parameter $\alpha_d$ represents the strength of the radial variation.

### A. Full 2-D solution

Before we consider the full 2-D problem, it is useful to plot stability boundaries from both the local peeling mode theory discussed in Sec. II and a naive application of ballooning theory, i.e., we do not concern ourselves with the inconsistencies in the higher order ballooning theory for the present—these will be addressed later in Sec. III B. We develop a ballooning solution to Eq. (30) by writing $u_m(x) \simeq e^{imk}u(x-M)$, where $k$ represents the standard ballooning phase angle, related to the radial wave number as discussed in Sec. I. As we shall restrict our consideration to ballooning stability in the first stable regime, we can take $k = 0$, in which case we write

$$u(z) = \int_{-\infty}^{\infty} y(\eta) e^{iz\eta}\, d\eta \tag{34}$$

and derive the leading order ballooning equation from Eq. (30)

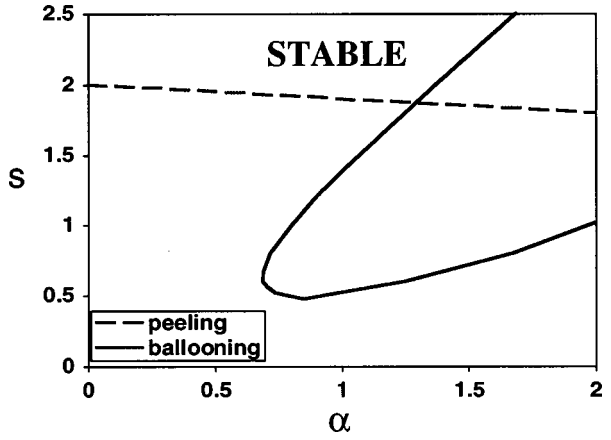


FIG. 2. The ballooning (full curve, fixed $k=0$) and peeling (dashed curve) marginal stability contours in the $s-\alpha$ plane for $d_m=-0.2$.

$$\frac{d}{d\eta}\left\{[1+h^2(\eta)]\,\frac{dy}{d\eta}\right\}+\alpha\Gamma y=0, \tag{35}$$

where

$$h=s\eta-\alpha\,\sin\,\eta, \tag{36}$$

$$\Gamma=\cos\,\eta+h\,\sin\,\eta+d_m, \tag{37}$$

and the boundary condition that $y\to 0$ as $|\eta|\to\infty$ is to be imposed. (It is straightforward to generate the ballooning equation for arbitrary $k$, but an unneccesary complication for the present model.) Apart from the magnetic well term, $d_m$, this equation corresponds to the standard $s-\alpha$ model. Using Eqs. (1), (27) and the equilibrium condition $\gamma=2-s$, we obtain the peeling mode stability boundary and from Eq. (35) we obtain the ballooning mode boundary; these two boundaries are shown in Fig. 2.

We turn now to the solution of the full 2-D system of equations. The numerical procedure follows a ''forward- and backsubstitution'' technique[21] for a vector $\mathbf{u}(x)$, whose elements are the $u_m(x)$; this treats $\Omega^2$ as an eigenvalue for a given choice of $s$ and $\alpha$. Values of $s$ and $\alpha$ for which $\Omega^2=0$ define marginal stability curves in the $s-\alpha$ diagram (although $\Omega$ is not a true mode frequency, it does have the property that $\Omega^2<0$ corresponds to instability, while $\Omega^2>0$ corresponds to stability). Rather than $s$, we shall use the edge current density parameter $\gamma=2j_\parallel/\langle j\rangle=2-s$. Figure 3 shows the variation of edge current density with $\alpha$ at marginal stability for $\Delta=0.005$, demonstrating that there can be two solutions for $\alpha$ for a given edge current density. The upper solution occurs just below the ballooning stability boundary, while the lower solution is close to the peeling mode boundary. This is in qualitative agreement with earlier studies of coupled peeling–ballooning modes, which considered $\Delta\ll 1$ and employed simpler models of the plasma equilibrium than that developed here.[22–24] A comparison between the full 2-D calculation of the marginal stability curve and those derived for the individual peeling and ballooning modes is shown in Fig. 4, which also shows the marginal stability curves for a range of other values of $\Delta$. For very low

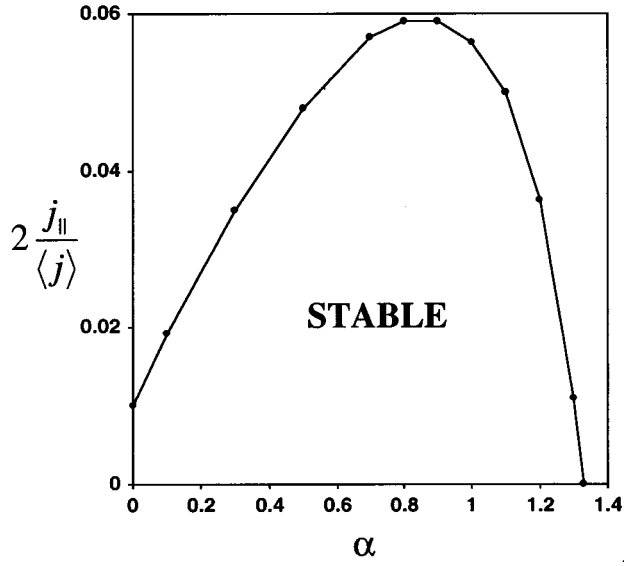


FIG. 3. The marginally stable edge current as a function of edge pressure gradient for parameters $\Delta=0.005$, $d_m=-0.2$, $\alpha_d=1$, $q_a\simeq 4$, $n=10$.

$\Delta$ (e.g., $\Delta=0.005$) and low edge current, the stability boundaries are described reasonably well by the peeling and ballooning mode boundaries. At higher current density, the ballooning and peeling modes couple and reduce the stable region. This effect was also predicted in the earlier analyses of coupled peeling–ballooning modes.[22–24] However, at larger $\Delta$ the peeling mode stability criterion is no longer an accurate prediction of the actual stability boundary. This is associated with two effects: (1) the stabilizing effect of the vacuum (neglected in the peeling analysis) becomes important and (2) there is a small amount of ''small'' solution in the peeling modelet which was neglected in the trial function

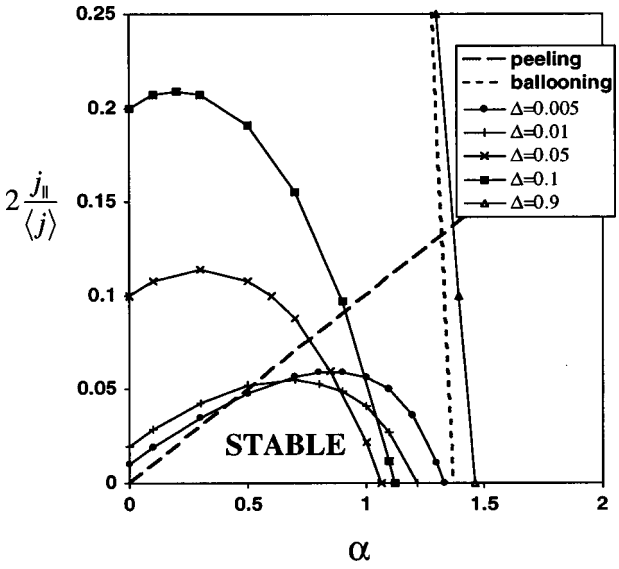


FIG. 4. The marginally stable edge current as a function of pressure gradient for a variety of $\Delta$ values, for parameters $d_m=-0.2$, $\alpha_d=1$, $q_a\simeq 4$, $n=10$. The dashed curve shows the peeling mode stability criterion from Eq. (11) and the dotted curve is the $n=\infty$ ballooning boundary evaluated from Eq. (35).

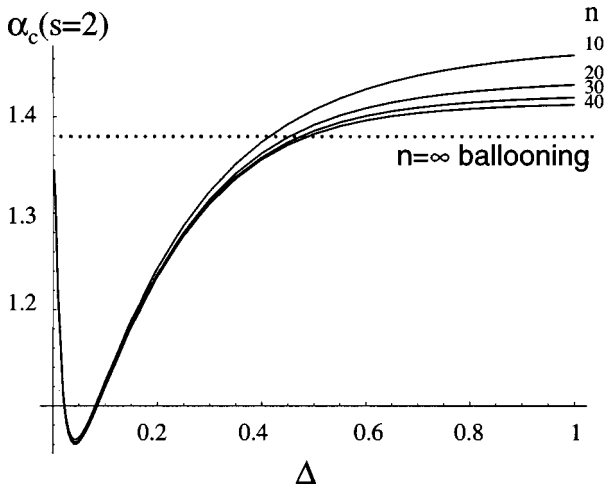


FIG. 5. The effect of $\Delta$ on the critical edge pressure gradient for instability in the absence of edge current (i.e., $s=2$).

used to derive Eq. (10) (i.e., $a_+$ is small, but not zero). In fact, it is possible to solve the $\alpha=0$ limit of the system of equations (30) and (31) analytically to derive the minimum current required to destabilize the peeling mode as a function of $\Delta$

$$\frac{j_\parallel}{\langle j\rangle}=\Delta, \tag{38}$$

which agrees with the results of the 2-D calculation. For large $\Delta$, approaching unity, the peeling mode plays essentially no role in the edge stability, as can be seen from the stability boundary for $\Delta=0.9$ shown in Fig. 4: This is close to the ballooning boundary. In fact, in the absence of edge current, the behavior of the ballooning mode boundary with $\Delta$ is rather interesting. For low values of $\Delta$ ($\Delta\lesssim 0.05$) the coupling between the ballooning mode and peeling mode increases with $\Delta$ and the critical $\alpha$ for instability in the absence of edge current reduces. However, for $\Delta\gtrsim 0.05$, the coupling between the modes weakens and as $\Delta$ is increased towards unity, the critical $\alpha$ rises above the $n=\infty$ ballooning limit. This is illustrated in Fig. 5 which shows the variation of the critical $\alpha$ required for instability in the absence of edge current. We note that, despite our observation in the Introduction that the conventional higher order ballooning theory is not valid at the plasma edge, the stability boundary does appear to be governed by the leading order ballooning theory, at least when the peeling mode is not important. We shall return to this in the following subsection.

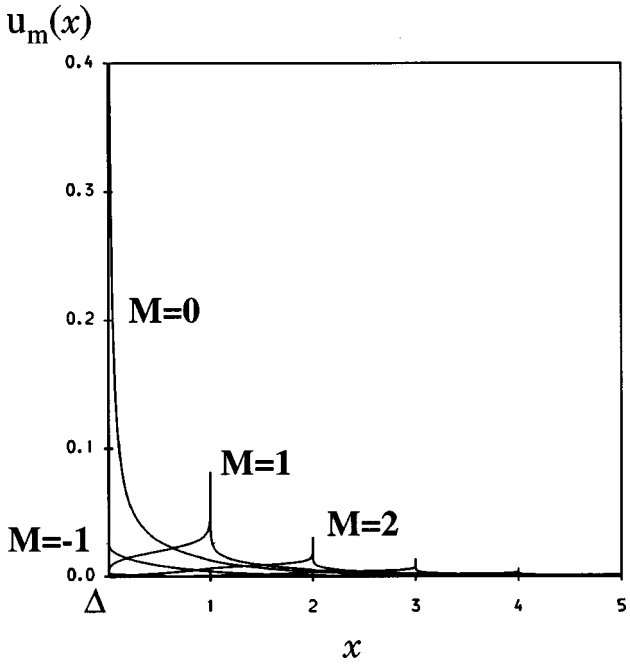


FIG. 6. The mode structure of the peeling mode branch of the 2-D solution using the same parameters as Fig. 4 ($\Delta=0.01$) for $\alpha=1.0$, $s=1.945$.

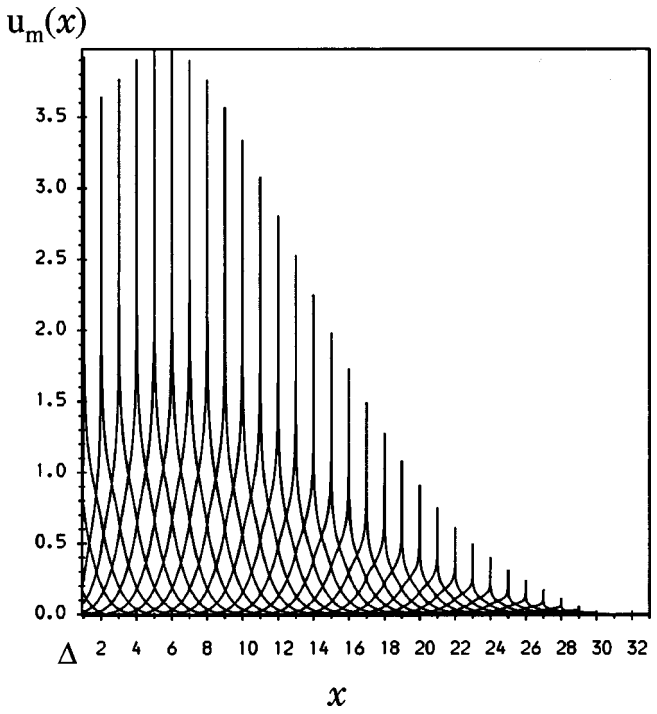


FIG. 7. The mode structure of the ballooning mode branch of the 2-D solution using the same parameters as Fig. 4 ($\Delta=0.9$) but using $n=40$ (which increases the number of coupled $u_m$) for marginally stable $\alpha=1.41$, $s=2.0$.

It is interesting to look at the radial structure of these modes, which have very different forms depending on the proximity of $\alpha$ to the ideal $n=\infty$ ballooning limit. Up to quite large $\alpha$, $\alpha\sim 1$, only a relatively few poloidal Fourier harmonics are coupled. This is illustrated in Fig. 6 which shows the mode structure for a peeling-type mode with $\Delta=0.01$ at $\alpha=1$. To investigate the mode structure close to the ballooning limit, we consider a larger value of $\Delta$, $\Delta=0.9$, to suppress the peeling mode: Figure 7 shows a dramatic increase in the number of Fourier harmonics which couple to form the ballooning mode structure. Note that this ballooning instability is much more radially extended than the peeling mode, and spans many rational surfaces; we shall consider this further in the following subsection.

### B. Edge ballooning theory

As discussed in the Introduction, conventional ballooning mode theory[8] is not valid at the plasma edge. The reason that it fails is that the ''local'' eigenvalue $\omega^2$ varies essentially linearly with radius, while conventional ballooning theory requires the eigenvalue to have a local minimum in radius. In this subsection we describe a modified ballooning formalism which accommodates this situation and is valid at the plasma edge.

We start with the Euler equation, derived from Eq. (20), describing the MHD stability of a general tokamak plasma to high $n$ modes

$$JBk_{\|}\left\{\frac{1}{JR^2B_p^2}\left[1-\left(\frac{R^2B_p^2}{B}\right)^2\frac{1}{n^2}\frac{\partial^2}{\partial\psi^2}\right]JBk_{\|}X\right\}+\frac{2Jp'}{B^2}\frac{\partial}{\partial\psi}\left(p+\frac{B^2}{2}\right)X-\frac{iIp'}{B^4}\frac{\partial B^2}{\partial\chi}\frac{1}{n}\frac{\partial X}{\partial\psi}=0 \tag{39}$$

and we neglect the surface term, which is not important for ballooning modes that penetrate deep into the plasma (see Fig. 7). We now apply the ballooning transformation

$$X=\sum_m e^{-im\chi}\int_{-\infty}^{\infty}d\eta\, e^{im\eta}F(\psi,\eta)\times\exp\left(-in\int_k^{\eta}\nu\, d\eta'\right), \tag{40}$$

whose value relies on the slow radial variation of the equilibrium from one rational surface to the next. Clearly this fails at the plasma edge, where the pressure gradient changes discontinuously from a finite value inside the plasma to zero outside, for example. However, we note that only a relatively few Fourier ''modelets'' extend to the plasma edge, so we neglect the effect of the edge discontinuity and simply map the periodic variable $\chi$ to the infinite variable $\eta$, with the periodicity boundary condition replaced by the boundary condition that the ballooning transformed displacement $F\rightarrow 0$ as $|\eta|\rightarrow\infty$ (i.e., the conventional boundary condition in ballooning theory). We define a new radial coordinate $y=n^{2/3}(\psi-\psi_a)$, where $\psi_a$ is proportional to the poloidal flux at the plasma edge, and assume $\partial F/\partial y=O(1)$ (to be justified *a posteriori*). Equation (39) then becomes

$$\frac{\partial}{\partial\eta}\left\{\frac{1}{JR^2B_p^2}\left[\frac{1}{n^{2/3}}\frac{\partial^2}{\partial y^2}-\frac{2i\zeta'}{n^{1/3}}\frac{\partial}{\partial y}-(\zeta')^2\right]\right\}\times\frac{\partial F}{\partial\eta}+\Lambda\left[\frac{2J}{B^2}p'\frac{\partial}{\partial\psi}\left(p+\frac{B^2}{2}\right)-i\frac{Ip'}{B^4}\frac{\partial B^2}{\partial\chi}\left(\frac{1}{n^{1/3}}\frac{\partial}{\partial y}-i\zeta'\right)\right]F=0. \tag{41}$$

We recall a prime denotes a derivative with repect to $\psi$ and we have defined

$$\zeta'=\int_k^{\eta}\nu'\, d\eta. \tag{42}$$

Note that we have introduced a ''fictitious'' eigenvalue $\Lambda$, which has no particular physical significance but provides a useful device to obtain the marginal stability condition; at the end of the calculation we apply the ''dispersion relation''

$$\Lambda=1 \tag{43}$$

which is the condition that the actual pressure gradient corresponds to the marginal value.

We now expand

$$F=F_0+n^{-1/3}F_1+n^{-2/3}F_2+\cdots \tag{44}$$

and introduce a local eigenvalue

$$\lambda(\psi,k)=\Lambda+O(n^{-2/3}). \tag{45}$$

The Euler equation can now be written, collecting powers of $n^{-1/3}$:

$$[L_0+n^{-1/3}L_1+n^{-2/3}L_2][F_0+n^{-1/3}F_1+n^{-2/3}F_2\cdots]+[\lambda+(\Lambda-\lambda)][M_0+n^{-1/3}M_1][F_0+n^{-1/3}F_1+n^{-2/3}F_2\cdots]=0, \tag{46}$$

where the operators take similar forms to those of the conventional ballooning theory[8]

$$\begin{aligned}
&L_0=\frac{\partial}{\partial\eta}\left[\frac{1}{JR^2B_p^2}\left[1+\left(\frac{R^2B_p^2}{B}\right)^2(\zeta')^2\right]\frac{\partial}{\partial\eta}\right],\\
&M_0=\frac{2J}{B^2}p'\frac{\partial}{\partial\psi}\left(p+\frac{B^2}{2}\right)-\frac{Ip'}{B^4}\frac{\partial B^2}{\partial\chi}\zeta',\\
&L_1=i\hat{L}_1\frac{\partial}{\partial y},\quad M_1=i\hat{M}_1\frac{\partial}{\partial y},\\
&\hat{L}_1=-\frac{1}{\nu'(k)}\frac{\partial L_0}{\partial k},\quad \hat{M}_1=-\frac{1}{\nu'(k)}\frac{\partial M_0}{\partial k},\\
&L_2=\hat{L}_2\frac{\partial^2}{\partial y^2},\quad \hat{L}_2=-\frac{1}{2\nu'(k)}\frac{\partial}{\partial k}\left(\frac{1}{\nu'(k)}\frac{\partial L_0}{\partial k}\right).
\end{aligned} \tag{47}$$

We now solve this system order by order in $n^{-1/3}$; to leading order

$$L_0F_0+\lambda M_0F_0=0. \tag{48}$$

Noting that $L_0$ is a differential operator in $\eta$ alone, and depends only parametrically on $\psi$ and $k$, we can write $F_0=A(y)f_0(\psi,\eta)$ and $\lambda=\lambda(k,\psi)$. The form of $A(y)$, the value of $k$, and the relation between $\Lambda$ and $\lambda$ are all determined at higher order, as we now demonstrate. Thus, proceding to $O(n^{-1/3})$, we have

$$F_1=\frac{dA}{dy}f_1, \tag{49}$$

where

$$L_0f_1+\lambda M_0f_1+i\hat{L}_1f_0+i\lambda\hat{M}_1f_0=0. \tag{50}$$

A solubility condition is derived by multiplying Eq. (50) by $f_0$ and integrating over $\eta$

$$\langle f_0(L_0+\lambda M_0)f_1\rangle+i\langle f_0(\hat{L}_1+\lambda\hat{M}_1)f_0\rangle=0, \tag{51}$$

where we have defined

$$\langle \cdots \rangle = \int_{-\infty}^{\infty} \cdots d\eta. \tag{52}$$

Note that the first term in Eq. (51) is zero as a consequence of the Hermitian nature of $L_0$ and $M_0$ and Eq. (48). Differentiating the zeroth order result

$$\langle f_0(L_0+\lambda M_0)f_0\rangle = 0 \tag{53}$$

with respect to $k$ we find that Eq. (51) can be expressed in the form familiar from conventional ballooning theory, i.e.,

$$\frac{\partial \lambda(\psi,k)}{\partial k} = 0 \tag{54}$$

which determines the value of $k$.

We now proceed to the $O(n^{-2/3})$ equation, which has the solubility condition

$$[i\langle f_0(\hat{L}_1+\lambda\hat{M}_1)f_1\rangle + \langle f_0\hat{L}_2 f_0\rangle]\frac{d^2A}{dy^2} + n^{2/3}(\Lambda-\lambda)$$

$$\times\langle f_0 M_0 f_0\rangle A = 0. \tag{55}$$

This condition provides the equation for the envelope function $A$, with the relationship between $\Lambda$ and $\lambda$ determined by the eigenvalue condition. Using results derived from differentiating Eq. (53) with respect to $k$, together with Eq. (50), the envelope equation can be simplified

$$\frac{\partial^2\lambda}{\partial k^2}\frac{d^2A}{dy^2} + 2[\nu'(k)]^2[n^{2/3}(\Lambda-\lambda)-\lambda' y])A = 0, \tag{56}$$

where we have Taylor expanded $\lambda$ about $y=0$,

$$\lambda(\psi) = \lambda(\psi_a) + \lambda' \frac{y}{n^{2/3}}. \tag{57}$$

This is an Airy equation,[15] and clearly for $\lambda'<0$ (which corresponds to the plasma becoming more unstable as the edge is approached) we must choose

$$\frac{\partial^2\lambda}{\partial k^2} > 0, \tag{58}$$

i.e., the value of $k$ from the solution of Eq. (54) that maximizes instability (note, $y$ becomes increasingly negative into the plasma). Thus the solution for the general equilibrium case is the Airy function[15]

$$A(y) = \mathrm{Ai}\left[\left(\frac{2[\nu'(k)]^2\lambda'}{\lambda_{kk}}\right)^{1/3}\left[y + \frac{n^{2/3}}{\lambda'}(\lambda_a-\Lambda)\right]\right], \tag{59}$$

where $\lambda_{kk} \equiv \partial^2\lambda/\partial k^2$ and $\lambda_a \equiv \lambda(\psi_a)$. To obtain the eigenvalue condition, we must specify the value of $A(y)$ at the plasma surface ($y=0$). Neglecting the coupling to the peeling mode and other external modes, we expect $A(y=0)=0$; this condition leads to the dispersion relation

$$\lambda_a = 1 - \left(\frac{\lambda_{kk}}{2}\right)^{1/3}\left[-\frac{9\pi}{8}\frac{\lambda'}{nq'}\right]^{2/3}. \tag{60}$$

We note that the envelope $A$ does indeed vary on the length scale associated with $y$ (as assumed in the $n^{-1/3}$ ordering), so that the ballooning mode penetrates a distance $\sim n^{1/3}$ rational surfaces into the plasma; also the correction to the leading order ($n=\infty$) ballooning eigenvalue is $O(n^{-2/3})$. These results can be compared to the conventional ballooning mode, which spans $\sim n^{1/2}$ rational surfaces, and has a correction to the leading order ballooning eigenvalue which is smaller, i.e., $O(n^{-1})$.

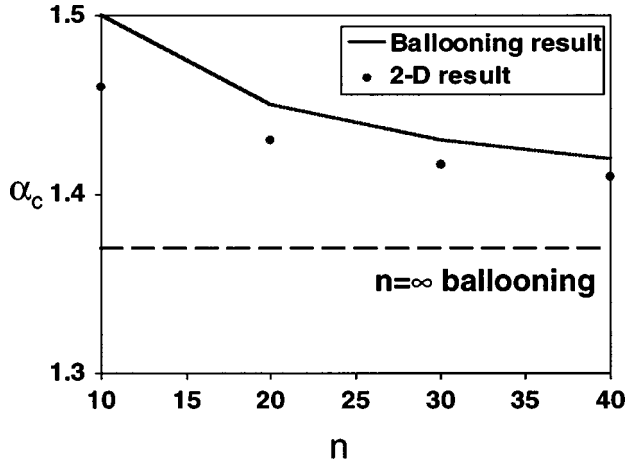


FIG. 8. Comparison of the critical $\alpha_c$ for ballooning stability at $s=2$ for the same parameters as used for Fig. 4 ($\Delta=0.9$), plotted as a function of $n$. The full curve is the solution to Eq. (62), taking the finite $n$ correction into account, while the dots are the solutions to the full 2-D Eq. (30).

The ballooning analysis results can be compared with the 2-D $s-\alpha$ model results described in the previous subsection. For this comparison it is convenient to write

$$\lambda' = \frac{q'\alpha_d}{qs}\frac{\partial\lambda}{\partial\alpha}, \tag{61}$$

where the radial variation in the pressure gradient parameter $\alpha$ is characterized by $\alpha_d$, as for the 2-D model [see Eq. (33)]. The ballooning equation for this model has been derived in Eq. (35), with $\alpha \to \lambda_a\alpha$ to take account of the fictitious eigenvalue $\lambda_a$, i.e.,

$$\frac{d}{d\eta}\left\{[1+h^2(\eta)]\frac{dy}{d\eta}\right\} + \lambda_a\alpha\Gamma y = 0 \tag{62}$$

with $h = s(\eta-k) - \alpha\sin\eta$ and $\Gamma$ as defined in Eq. (37). Thus the technique to derive the marginal stability curves in the $s-\alpha$ plane, retaining finite $n$ corrections, is as follows. First we fix $s$ and guess the critical $\alpha$ for marginal stability for this $s$. Equation (62) is then solved to derive $\lambda_a$, $\lambda_{kk}$ and $\lambda_\alpha (\equiv \partial\lambda/\partial\alpha)$. We then iterate on $\alpha$ until Eq. (60) is satisfied for $\lambda_\alpha$; clearly for $n\to\infty$, the marginally stable path in the $s-\alpha$ plane is given by $\lambda_a = 1$. In Fig. 8 we fix $s=2$ (i.e., no edge current density) and compare the results for the marginally stable $\alpha_c$ obtained from the full 2-D eigenvalue code with those obtained from the ballooning analysis described above. The results are plotted for a range of $n$, and are broadly in agreement: The difference between the two results scales approximately as $1/n$. In particular, in Fig. 9 we show that the critical $\alpha$ calculated from the 2-D code does indeed have a correction $\sim n^{-2/3}$, and that an $n^{-1}$ correction predicted by conventional ballooning theory does not describe the results from the 2-D code.

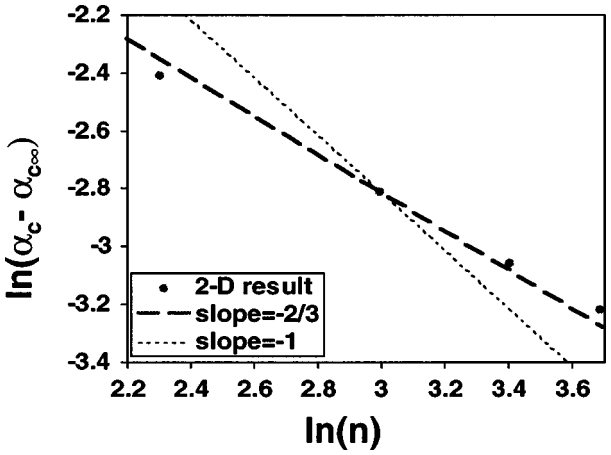


FIG. 9. Demonstration that the 2-D result for $\alpha_c$ varies as $n^{-2/3}$; the conventional ballooning theory result scales as $n^{-1}$ which clearly does not describe the 2-D calculation (parameters as for Fig. 8).

As a final comparison between the ballooning results and those from the full 2-D calculation, we plot the radial envelope of the eigenfunction predicted by the Airy function solution to Eq. (56) as the dashed curve in Fig. 10. This solution has the boundary condition $A(x)=0$ at the end point, for consistency with the 2-D solutions with cut-off $M=26$ for $n=20$ and $M=30$ for $n=40$ (since this is a finite end point, it introduces a small amount of Bi,[15] the second solution of the Airy equation). We see that good agreement can be obtained if the ballooning eigenfunction is shifted by two rational surfaces towards the plasma edge, which is consistent with the $O(1/n)$ difference between the 2-D and high $n$ ballooning theory eigenvalues illustrated in Fig. 8.

## IV. SUMMARY

We have calculated marginal stability curves for high $n$ MHD instabilities at the plasma edge. Two types of instabilities have been identified from the 2-D calculation of the marginal stability boundaries: One is a current-driven peeling mode, and one is a pressure-driven ballooning mode. The peeling mode is dominated by a single poloidal Fourier harmonic associated with the first rational surface outside the plasma, but this can drive several ''sideband'' harmonics in the plasma edge region. The number of coupled harmonics appears to be most sensitive to $\alpha$; as the pressure gradient is increased towards the ballooning instability boundary there is a sudden dramatic increase in the number of harmonics which are coupled to form the ballooning mode. Analytic calculations demonstrate that the ballooning mode has the same $n=\infty$ stability boundary as that predicted by the conventional ballooning equation when the coupling to the peeling mode is not important (e.g., when the last internal rational surface is close to the plasma edge). However, the edge ballooning mode has a larger, stabilizing, finite $n$ correction, proportional to $n^{-2/3}$, than conventional ballooning theory would predict. Furthermore, the individual poloidal Fourier harmonics are coupled and have an Airy function envelope, while conventional ballooning theory would predict a Gaussian envelope. The ballooning mode penetrates a distance $\Delta r \sim (nqs)^{-2/3}a$ into the plasma, i.e., a fraction $\sim 5\%$ of the plasma minor radius for typical tokamak parameters ($n=10$, $q=4$, $s=2$), which is comparable to a typical H-mode pedestal width.

While we have considered a model system based on a limiter tokamak equilibrium, the features of the instabilities we have examined offer explanations of several features observed in separatrix plasma H-modes. An example is illus-

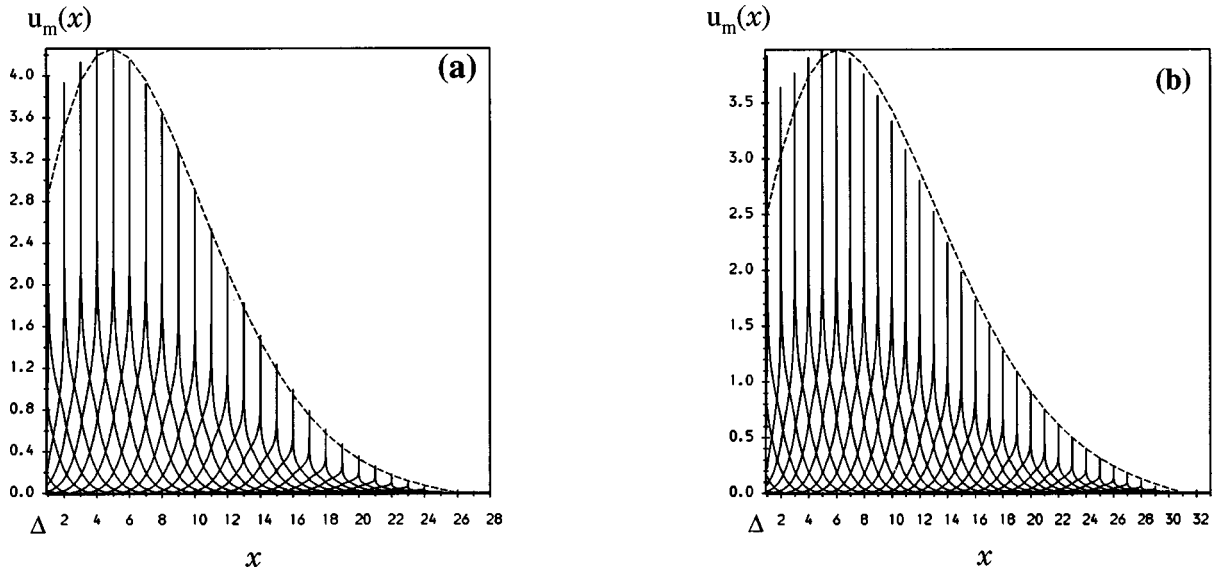


FIG. 10. The Airy function envelope calculated from the solution to Eq. (56) with boundary condition (a) $A(x=27)=0$ and (b) $A(x=31)=0$ (dashed curves) for consistency with the 2-D solution (full curves) with cut-off (a) $M=26$ and (b) $M=30$. The equilibrium parameters are those of Fig. 4 for $\Delta=0.9$. Two values of $n$ are shown: (a) $n=20$ for which the Airy function has been shifted by two rational surfaces towards the plasma surface to obtain a good fit and (b) $n=40$ for which the Airy function has been shifted by 2.5 surfaces.

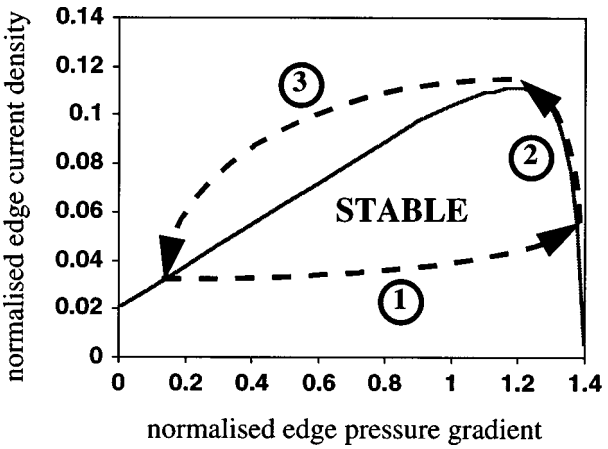


FIG. 11. Plasma parameter evolution during ELM cycle (dashed curve) relative to edge MHD stability boundary (full curve): edge pressure gradient rises up to ballooning limit (1), which restricts further increase; edge current rises due to Ohmic and bootstrap currents (2) up to top corner of stability boundary; plasma instability flushes out pressure, enhancing the instability and resulting in a crash of the edge pressure gradient and current (3), which is interpreted as the ELM crash. The cycle repeats with further heating.

trated by Eq. (17) which describes stability to the peeling mode. If the edge plasma collisionality is high, so that the fraction of trapped particles $f_t$ is small, then stability to the peeling mode can be achieved by raising the edge pressure gradient. It is difficult to imagine that an edge transport barrier can form while the peeling instability is active, so that a necessary condition for an L–H mode transition is that the peeling mode be stabilized: This would correspond to a power threshold. However, if the edge collisionality falls once the H-mode has been accessed, so that the edge bootstrap current is enhanced through $f_t$, the peeling mode would become unstable, resulting in a collapse of the transport barrier. It is interesting to note that there is a dramatic loss in confinement in low collisionality Joint European Torus (JET)[25] discharges, but that this can be prevented by a current ramp-down.[26] In addition, COMPASS-D[12] cannot access the H-mode if the density is low, which may correspond to low edge collisionality.

When coupled with the ballooning mode, the peeling mode also provides a model for Type I ELMs. The conceptual picture is illustrated schematically in Fig. 11. First, the peeling boundary is crossed and the resulting improvement in edge confinement causes the pressure gradient to rise to the ballooning limit, where it is held (1). Meanwhile, the current increases (usually on a slower, resistive time scale) due to the rise in bootstrap and Ohmic currents and the plasma reaches the top corner of the stable ''triangle'' (2). As the stability boundary is crossed, there is a loss of edge confinement so that the edge pressure gradient drops, further destabilizing the peeling mode. Thus there is a rapid collapse of the pressure gradient (3), which we interpret as the Type I ELM crash. Note that the plasma can ''sit'' against the ballooning limit for some time before the edge current builds to a sufficient level to cause the ELM. This feature has been observed in several tokamaks.[5–7]

To make more quantitative statements about the role of edge MHD and ELMs requires the particular features of plasma flow (driven by the radial electric field in H-mode discharges) and separatrix geometry to be taken into account. A sheared flow is likely to have a significant stabilizing effect on the ballooning mode and will also modify its radial structure, for example.[27] There are two clear differences between limiter and separatrix geometry relevant to the peeling mode stability analysis. In the separatrix geometry, $q \to \infty$ at the separatrix so that, first, one can always place the reference rational surface inside the plasma and, second, one cannot neglect the variation of $q$ across the mode width. A third complication with the separatrix geometry is that there are many (indeed, formally an infinite number) rational surfaces between the reference rational surface and the plasma edge, which may complicate the local peeling stability analysis as developed in the Appendix. An interesting feature of separatrix geometry is that the dominant contribution to Eq. (1) from the Pfirsch–Schlüter current will originate from poloidal angles in the vicinity of the X point. Thus an inboard X point is expected to be strongly stabilising for peeling modes because the Pfirsch–Schlüter current is negative there, while an outboard X point will be destabilizing. Work is under way to address these geometrical and plasma flow issues.

## ACKNOWLEDGMENTS

R.L.M. would like to thank UKAEA Fusion, Culham Science Centre, for their hospitality during his visit.

This work was funded jointly by the UK Department of Trade and Industry and Euratom, and by the US Department of Energy under Grant No. DE-FG03-95ER54309.

## APPENDIX: PEELING MODE ENERGY PRINCIPLE

In this appendix we derive the peeling mode energy principle. While this appears elsewhere in the literature it is useful to repeat the calculation in full here as we make reference to specific details and notation in the main body of this paper.

Lortz demonstrated that the vacuum contribution to the change in potential energy associated with a localized surface mode could be neglected;[9] we therefore only consider the change in energy associated with the plasma. This has been calculated in the convenient form[8]

$$\delta W = \frac{1}{2}\int J\, d\psi\, d\chi\, d\phi \left\{ \frac{B^2}{R^2 B_p^2}\,|k_\parallel X|^2 + \frac{R^2}{J^2}\left|\frac{\partial U}{\partial \chi}\right. \right. - I\,\frac{\partial}{\partial \psi}\left(\frac{JX}{R^2}\right)\Bigg|^2 + B_p^2\left| inU + \frac{\partial X}{\partial \psi} - \frac{j_\phi X}{RB_p^2}\right|^2 - 2K|X|^2 + \gamma_s p\left|\frac{1}{J}\frac{\partial}{\partial \psi}(JX) + inU + iBk_\parallel Z\right|^2 \Bigg\}, \tag{A1}$$

where we have defined the perturbed plasma displacement ($\sim e^{in\phi}$)

$$\boldsymbol{\xi} = \frac{\xi_\psi}{RB_p}\nabla\psi + \frac{\xi_\chi}{B_p}(\nabla\phi \times \nabla\psi) + R\xi_\phi \nabla\phi \tag{A2}$$

and expressed the components of $\boldsymbol{\xi}$ in terms of

$$X=RB_p\xi_\psi, \quad U=\left(\frac{\xi_\phi}{R}-\frac{I}{R^2B_p}\,\xi_\chi\right), \quad Z=\frac{\xi_\chi}{B_p}. \tag{A3}$$

$R$ is the major radius, $p$ the pressure, $B_p$ the poloidal magnetic field strength, and $I=RB_\phi$, where $B_\phi$ is the toroidal magnetic field strength. The coordinate system we use comprises the toroidal angle $\phi$, the poloidal flux $\psi$ (increasing towards the plasma edge) and a poloidal angle $\chi$ (defined so that the system is orthogonal), with Jacobian $J$. We have also defined the ratio of specific heats $\gamma_s$ and

$$j_\phi=-Rp'-\frac{II'}{R}=\frac{R}{J}\frac{\partial}{\partial\psi}(JB_p^2), \tag{A4}$$

$$K=\frac{II'}{R^2}\frac{\partial}{\partial\psi}(\ln R)+\frac{j_\phi}{R}\frac{\partial}{\partial\psi}\ln(JB_p), \tag{A5}$$

$$ik_\parallel=\frac{1}{JB}\left(\frac{\partial}{\partial\chi}+in\nu\right), \tag{A6}$$

with $\nu=IJ/R^2$, $j_\phi$ the toroidal current density, $k_\parallel$ is a parallel wavenumber, and prime denoting a derivative with respect to $\psi$. Neglecting the vacuum energy, the integral is over the plasma volume.

Our goal is to determine an eigenmode equation by deriving the Euler equation which minimizes $\delta$W. As the last term in $\delta$W is positive definite, $Z$ is to be chosen so that this is zero. Thus it remains to minimize

$$\delta W=\frac{1}{2}\int J\,d\psi\,d\chi\,d\phi\left\{\frac{B^2}{R^2B_p^2}\,|k_\parallel X|^2+\frac{R^2}{J^2}\left|\frac{\partial U}{\partial\chi}-I\frac{\partial}{\partial\psi}\left(\frac{JX}{R^2}\right)\right|^2+B_p^2\left|inU+\frac{\partial X}{\partial\psi}-\frac{j_\phi X}{RB_p^2}\right|^2-2K|X|^2\right\} \tag{A7}$$

with respect to $X$ and $U$. To do this we introduce the small parameter $\epsilon$ and define a new ''length'' scale

$$x=\frac{(\psi-\psi_0)}{\epsilon}, \tag{A8}$$

where $x=0$ is the rational surface defined by $q=m/n$ and $x=1$ the plasma edge. [Note that this rapid radial length scale is not to be confused with that used in the main body of the text, which is defined in Eq. (26).] We then expand

$$\begin{aligned} X&=X_0+\epsilon X_1+\epsilon^2X_2+\cdots,\\ U&=U_0+\epsilon U_1+\epsilon^2U_2+\cdots,\\ \delta W&=\epsilon^{-1}\delta W^{(-1)}+\delta W^{(0)}+\epsilon\delta W^{(1)}+\cdots, \end{aligned} \tag{A9}$$

assuming $\partial X/\partial x\sim\partial U/\partial x\sim O(1)$, while derivatives of equilibrium quantities with respect to $x$ are $O(\epsilon)$. Thus in leading order we have

$$\delta W^{(-1)}=\frac{1}{2}\int J\,dx\,d\chi\,d\phi\,B_0^2\left|\frac{\partial X_0}{\partial x}\right|^2 \tag{A10}$$

and we choose

$$X_0=0\Rightarrow\delta W^{(-1)}=0. \tag{A11}$$

This choice also results in $\delta W^{(0)}=0$, so we proceed to the $O(\epsilon)$ contribution, which is

$$\delta W^{(1)}=\frac{1}{2}\int J\,dx\,d\chi\,d\phi\left(\frac{R^2}{J^2}\left|\frac{\partial U_0}{\partial\chi}-I\frac{\partial}{\partial x}\left(\frac{JX_1}{R^2}\right)\right|^2+B_p^2\left|inU_0+\frac{\partial X_1}{\partial x}\right|^2\right). \tag{A12}$$

Thus we take $X_1$ and $U_0$ to satisfy

$$\frac{\partial X_1}{\partial x}=-inU_0, \quad \frac{\partial U_0}{\partial\chi}=\nu_0\frac{\partial X_1}{\partial x}, \tag{A13}$$

where the equilibrium value with subscript zero indicates that it is to be evaluated on the rational surface. Combining the results from Eq. (A13), we find

$$\mathbf{B}_0\cdot\nabla X_1=0 \tag{A14}$$

so that $X_1$ is constant along a field line (i.e., the mode is flutelike). Equation (A13) implies $\delta W^{(2)}=0$, so we proceed to evaluate $\delta W^{(3)}$

$$\begin{aligned}\delta W^{(3)}=\frac{1}{2}\int J\,dx\,d\chi\,d\phi\Bigg\{&\frac{B_0^2}{R_0^2B_p^2}\,|k_\parallel X_1|^2-2K|X_1|^2\\&+\frac{R^2}{J^2}\left|\frac{\partial U_1}{\partial\chi}-\nu\frac{\partial X_2}{\partial x}-x\frac{\partial}{\partial\psi}\left(\frac{IJ}{R^2}\right)\frac{\partial X_1}{\partial x}\right.\\&\left.-I\frac{\partial}{\partial\psi}\left(\frac{J}{R^2}\right)X_1\right|^2+B_p^2\left|inU_1+\frac{\partial X_2}{\partial x}\right.\\&\left.-\frac{j_\phi}{RB_p^2}X_1\right|^2\Bigg\},\end{aligned} \tag{A15}$$

where we have dropped the suffix from equilibrium quantities. This is to be minimized with respect to $U_1$ and $X_2$, leaving an expression for $\delta W^{(3)}$ involving only $X_1$; this is our goal. Making use of $k_\parallel X_1=0$, $\delta W^{(3)}$ can be expressed in the more convenient form

$$\delta W^{(3)}=\frac{1}{2}\int J\,dx\,d\chi\,d\phi\left\{B^2\left|\frac{\partial X_2}{\partial x}-\frac{B_\phi^2A}{B^2}-\frac{B_p^2C}{B^2}\right|^2+\frac{B_p^2B_\phi^2}{B^2}\,|A-C|^2+D\right\}, \tag{A16}$$

where

$$A=\frac{1}{\nu}\left[\frac{\partial U_1}{\partial\chi}-x\frac{\partial}{\partial\psi}\left(\frac{IJ}{R^2}\right)\frac{\partial X_1}{\partial x}-I\frac{\partial}{\partial\psi}\left(\frac{J}{R^2}\right)X_1\right], \tag{A17}$$

$$C=-inU_1+\frac{j_\phi}{RB_p^2}X_1, \tag{A18}$$

$$D=-2K_0|X_1|^2. \tag{A19}$$

The first term is positive-definite, and we can minimize $\delta W^{(3)}$ by choosing $X_2$ so that this is zero. This leaves

$$\delta W^{(3)}=\frac{1}{2}\int J\,dx\,d\chi\,d\phi\left\{\frac{R^2B_p^2}{J^2B^2}\left|\frac{\partial U_1}{\partial\chi}+in\nu U_1-\frac{\partial}{\partial\psi}\left(\frac{IJ}{R^2}\right)x\,\frac{\partial X_1}{\partial x}-I\,\frac{\partial}{\partial\psi}\left(\frac{J}{R^2}\right)X_1-\frac{\nu j_\phi}{RB_p^2}\,X_1\right|^2-2K|X_1|^2\right\}. \tag{A20}$$

In this case we cannot simply choose $U_1$ so that the first term is zero, as this would lead to a solution which violates periodicity constraints. We therefore consider the Euler–Lagrange equation, which becomes

$$\left(\frac{\partial}{\partial\chi}+in\nu\right)\left[\frac{R^2B_p^2}{JB^2}\left(\frac{\partial U_1}{\partial\chi}+in\nu U_1-\frac{\partial}{\partial\psi}\left(\frac{IJ}{R^2}\right)x\,\frac{\partial X_1}{\partial x}-I\,\frac{\partial}{\partial\psi}\left(\frac{J}{R^2}\right)X_1-\frac{\nu j_\phi}{RB_p^2}\,X_1\right)\right]=0. \tag{A21}$$

Performing the first integration over $\chi$ determines the term in square brackets to a constant (on a flux surface) of integration, which itself is determined from the condition that $U_1$ be periodic in $\chi$. Substituting this result into Eq. (A20), one finds (after some algebra)

$$\delta W=\frac{\epsilon^3}{2}\int dx\left\{Px^2\left(\frac{d\xi}{dx}\right)^2+Q\xi^2+S\,\frac{d}{dx}\,(x\xi^2)\right\}, \tag{A22}$$

where $\xi\equiv X_1$ and

$$P=2\pi(q')^2\left[\oint\frac{JB^2}{R^2B_p^2}\,d\chi\right]^{-1},$$

$$Q=\frac{p'}{2\pi}\oint\frac{\partial J}{\partial\psi}\,d\chi-\frac{(p')^2}{2\pi}\oint\frac{J}{B_p^2}\,d\chi+Ip'\oint\frac{J}{R^2B_p^2}\,d\chi\left[\oint\frac{JB^2}{R^2B_p^2}\,d\chi\right]^{-1}\times\left[\frac{Ip'}{2\pi}\oint\frac{J}{R^2B_p^2}\,d\chi-q'\right], \tag{A23}$$

$$S=P+q'\oint\frac{j_\parallel B}{R^2B_p^2}\,Jd\chi\left[\oint\frac{JB^2}{R^2B_p^2}\,d\chi\right]^{-1}.$$

This is the final result of this Appendix, and is the result derived by Lortz. The integral to construct $\delta W$ is over the plasma volume and the coefficients $P$, $Q$, and $S$ are the flux surface averages indicated in Eq. (A23). Note in particular the surface term, with coefficient $S$, which characterizes the role of the edge parallel current, $j_\parallel$, in the peeling mode stability criterion (this term is absent for core instabilities, for which $\xi\to 0$ at the plasma edge).


[1] K. H. Burrell, Phys. Plasmas **4**, 1499 (1997).
[2] H. Biglari, P. H. Diamond, and P. W. Terry, Phys. Fluids B **2**, 1 (1990).
[3] M. Kotschenreuther, W. Dorland, Q. P. Liu, G. W. Hammett, M. A. Beer, S. A. Smith, A. Bondeson, and S. C. Cowley, in *Proceedings of the Sixteenth International Conference on Fusion Energy*, Montreal (International Atomic Energy Agency, Vienna, 1997), Vol. 2, p. 371.
[4] *Technical Basis for the ITER Interim Design Report, Cost Review and Safety Analysis* (International Atomic Energy Agency, Vienna, 1996)
[5] H. Zohm, W. Suttrop, H. J. de Blank, R. J. Buttery, D. A. Gates, J. A. Heikkinen, W. Herrmann, A. Kallenbach, T. Kass, M. Kaufmann, T. Kurki-Sonio, B. Kurzan, M. Maraschek, H. Reimerdes, F. Ryter, H. Salzmann, J. Schweinzer, J. Stober, ASDEX-Upgrade, ECRH, ICRH, and NBI teams, in *Proceedings of the Sixteenth International Conference on Fusion Energy*, Montreal (International Atomic Energy Agency, Vienna, 1997), Vol. 1, 439.
[6] G. Janeschitz, A. Hubbard, Yu. Igitkhanov, J. Lingertat, T. Osborne, H. D. Pacher, O. P. Pogutse, D. E. Post, M. Shimada, M. Sugihara, and W. Suttrop, in *Proceedings of the Twenty Fourth European Physical Society Conference on Controlled Fusion and Plasma Physics*, Berchtesgaden (European Physical Society, Petit-Lancy, 1997), Part III, 993.
[7] T. H. Osborne, R. J. Groebner, L. L. Lau, A. W. Leonard, R. Maingi, R. L. Miller, G. D. Porter, D. M. Thomas, and R. E. Waltz, in *Proceedings of the Twenty Fourth European Physical Society Conference on Controlled Fusion and Plasma Physics*, Berchtesgaden (European Physical Society, Petit-Lancy, 1997), Part III, 1101.
[8] J. W. Connor, R. J. Hastie and J. B. Taylor, Proc. R. Soc. London, Ser. A **365**, 1 (1979).
[9] D. Lortz, Nucl. Fusion **15**, 49 (1975).
[10] J. A. Wesson, Nucl. Fusion **18**, 97 (1978).
[11] R. J. Bickerton, J. W. Connor, and J. B. Taylor, Nature (London), Phys. Sci. **229**, 110 (1971).
[12] S. J. Fielding, J. D. Ashall, P. G. Carolan, A. Colton, D. Gates, J. Hugill, A. W. Morris, M. Valovic, and the COMPASS-D and ECRH teams, Plasma Phys. Controlled Fusion **38**, 1091 (1996).
[13] C. Mercier, Nucl. Fusion **1**, 47 (1960); Nucl. Fusion Suppl. **2**, 801 (1962).
[14] J. W. Connor, R. J. Hastie, and J. B. Taylor, Phys. Rev. Lett. **40**, 396 (1978).
[15] *Handbook of Mathematical Functions*, edited by M. Abramowitz and I. A. Stegun (Dover, New York, 1965), p. 441.
[16] A. H. Glasser, J. M. Greene, and J. L. Johnson, Phys. Fluids **18**, 875 (1975).
[17] A. H. Glasser, J. M. Greene, and J. L. Johnson, Phys. Fluids **19**, 567 (1976).
[18] H. Lütjens, A. Bondeson, and G. Vlad, Nucl. Fusion **32**, 1625 (1992).
[19] R. Fitzpatrick, C. G. Gimblett, and R. J. Hastie, Plasma Phys. Controlled Fusion **34**, 161 (1992); **34**, 1445 (1992).
[20] J. W. Connor, S. C. Cowley, R. J. Hastie, T. C. Hender, A. Hood, and T. J. Martin, Phys. Fluids **31**, 577 (1988).
[21] W. H. Press, B. P. Flannery, S. A. Teukolsky, and W. T. Vetterling, *Numerical Recipes* (Cambridge University Press, Cambridge, 1989).
[22] C. C. Hegna, J. W. Connor, R. J. Hastie, and H. R. Wilson, Phys. Plasmas **3**, 584 (1996).
[23] J. W. Connor and H. R. Wilson, in *Theory of Fusion Plasmas*, Varenna, edited by J. W. Connor, E. Sindoni, and J. Vaclavik (Editrice Compositori, Bologna, 1997) 441.
[24] H. R. Wilson and J. W. Connor, in *Proceedings of the Twenty Fourth European Physical Society Conference on Controlled Fusion and Plasma Physics*, Berchtesgaden (European Physical Society, Petit-Lancy, 1997), Part I, 289.
[25] P. H. Rebut, in *Proceedings of the Thirteenth International Conference on Controlled Fusion and Plasma Physics*, Washington (International Atomic Energy Agency, Vienna, 1991), Vol. 1, 27.
[26] M. F. F. Nave, G. T. A. Huysmans, B. Balet, B. de Esch, R. Gianella, C. Gowers, T. Jones, R. Konig, P. Lomas, V. V. Parail, F. Rimini, B. Schunke, and P. Thomas, in *Proceedings of the Twenty Fourth European Physical Society Conference on Controlled Fusion and Plasma Physics*, Berchtesgaden (European Physical Society, Petit-Lancy, 1997), Part I, 1.
[27] R. L. Miller, F. L. Waelbroeck, A. B. Hassam, and R. E. Waltz, Phys. Plasmas **2**, 3676 (1995).